FOVEAL WAVELET-BASED COLOR ACTIVE CONTOUR

Aldo Maalouf, Philippe Carré, Bertrand Augereau, Christine Fernandez-Maloigne

University of Poitiers
Signal-Image-Communication Laboratory
SP2MI-2 Bd Marie et Pierre Curie, PO Box 30179
86962 Futuroscope Chasseneuil, France
{maalouf, carre, augereau, fernandez}@sic.sp2mi.univ-poitiers.fr

ABSTRACT

A framework for active contour segmentation in vector-valued images is presented. It is known that the standard active contour is a powerful segmentation method, yet it is susceptible to weak edges and image noise. The proposed scheme uses foveal wavelets for an accurate detection of the edges singularities of the image. The foveal wavelets introduced by Mallat [1] are known by their high capability to precisely characterize the holder regularity of singularities. Therefore, image contours are accurately localized and are well discriminated from noise. Foveal wavelet coefficients are updated using the gradient descent algorithm to guide the snake deformation to the true boundaries of the objects being segmented. Thus, the curve flow corresponding to the proposed active contour holds formal existence, uniqueness, stability and correctness results in spite of the presence of noise where traditional snake approach may fail.

Index Terms— wavelet, active contour, segmentation, color images.

1. INTRODUCTION

Image segmentation is one of the basic problems in image analysis. Object detection has been studied since the early days of image analysis and computer vision and different approaches have been proposed. For a complete survey, the reader may refer to [2]. Active contour models can assist the process of object detection by providing high level information in the form of continuity constraints and minimum energy constraints related to the contour shape and image characteristics. The active contour method that has attracted most attention is known as Snake [3] [4] [5] [6] [7]. A snake is an energy minimizing curve which deforms its shape under the control of internal and external forces. These forces are specified so that the snake will hopefully achieve a minimal energy state when it matches the desired boundary to be detected.

In general, snakes use intensity gradient information as a feature to direct the curve deformation. However, intensity edges may appear in the scene without a material transition to support it. In addition, the intensity of the illumination may vary spatially over the scene causing a gradual change in intensity over the object's surface even though the surface is homogeneously painted.

Because intensity-based edge detectors cannot distinguish between various transition types, our attention is directed toward the use of multiscale approaches, namely the wavelets. The choice of which wavelet to use should be based on the precise contour localisation capability of that wavelet.

The foveal wavelets were first introduced in [1]. They mimic the non uniform distribution of photoreceptors on the retina. The visual resolution is highest at the center (fovea) of the retina, but falls off away from the fovea. This effect is modeled by foveal approximation spaces introduced in [1]. For example the piecewise constant foveal approximation space at the center $u \in \mathbb{R}$ is the set of all functions which are constant on $[u-2^{j+1}, u-2^{j})$ and $(u+2^{j}, u+2^{j+1}]$ for any $j \in \mathbb{Z}$. Projections in a foveal approximation space approximate functions with a resolution that decreases proportionally to the distance from u. Foveal approximation spaces are defined by dilating a finite family of foveal wavelets, which are not translated. Therefore, foveal wavelet coefficients give a pointwise characterization of singularities and precise approximations of piecewise regular functions are obtained by foveal approximations centered at singularity locations. As a result, the foveal wavelets can better localize edges than other wavelets.

Having well represented the edges, the foveal wavelet coefficients serve as weights that direct the snake curve deformation during the segmentation process. Therefore, an accurate edge detection is obtained.

The rest of the paper is organized as follows. In section 2, a review of the foveal wavelet is given. Section 3 aims to represent the traditional snake approach. In section 4 the foveal-wavelet snake approach is described. In section 5 experimental results are shown. Finally, section 6 presents some concluding remarks and perspectives.

2. FOVEAL WAVELETS

2.1. Review of the foveal wavelets

The contours are considered as one-dimensional singularities that move in the plane of the image. Foveal wavelets are orthogonal wavelets that are centered at the same location as if to absorb the singular behavior of the image [1]. These wavelets zoom on a single position u. It should be insured that the left and right indicators, $1_{[u,+\infty)}$ and $1_{(-\infty,u]}$, can be written as a linear combinations of foveal wavelets in order to be able to reconstruct singularities.

If $\mathbf{V}_u$ is the space generated by the foveal wavelet located at u, then the orthogonal projection of a function f in $\mathbf{V}_u$ is given by:

$$P_{V_u} f(t) = \sum_{j=-\infty}^{J} \sum_{k=1}^{2} \left\langle f, \psi_{j,u}^{k} \right\rangle \psi_{j,u}^{k}(t) \qquad (1)$$

Where ψ is the mother foveal wavelet. These wavelets are characterized by their ability to eliminate singularities located at u. If f is

This work was supported by the INTERREG III B PIMHAI project.

differentiable in a left and right neighborhood of u, but not in u then it has been shown in [1] that $f - P_{V_u} f$ is continuous at u and has a bounded derivative over a whole neighborhood of u. Therefore, the singularity of f at u is absorbed by the wavelet coefficients at u.
Singularities of f are entirely characterized by the foveal wavelet coefficient at u. It has been also shown in [1] that f is Lipschitz α at u if and only if $\left|\left\langle f, \psi^k_{j,u}\right\rangle\right| = O\left(2^{-\alpha(j+1/2)}\right)$. Singularities can be detected by computing

$$\varepsilon(u) = \sum_{j=-\infty}^{J} 2^{-2j} \sum_{k=1}^{2} \left|\left\langle f, \psi^k_{j,u}\right\rangle\right|^2 \tag{2}$$

If f has a Lipschitz regularity $\alpha < 1$ at u, and hence is not differentiable at u then $\varepsilon(u) \to +\infty$, but if f is Lipschitz regularity $\alpha > 1$ at u then $\varepsilon(u) < +\infty$. Singularities are thus detected from the amplitude of $\varepsilon(u)$.
We can, therefore, distinguish between noise singularities (negative Lipschitz component) and edge singularities from the amplitude of $\varepsilon(u)$.

2.2. Edge detection using foveal wavelets

The singularities of an image I are detected with one dimensional foveal wavelets, along each line and each column of the image. Detected singularities are chained together to form edge curves in two dimension.
Let $\{f(x_1, u_2)\}_{x_1 \in \mathbb{R}}$ be a horizontal scan line, where u_2 is fixed and x_1 varies. $\{f(x_1, u_2)\}_{x_1 \in \mathbb{R}}$ is decomposed over one-dimensional foveal wavelets. For each u we compute

$$\varepsilon_{u_2}(u) = \sum_{j} 2^{-2j} \sum_{k=1}^{2} \left|\left\langle f(x_1, u_2), \psi^k_{j,u}(x_1)\right\rangle\right|^2 \tag{3}$$

Any singularity corresponds to a point u_1 where $\varepsilon_{u_2}(u)$ is locally maximum when u varies. This singularity is located in the image plane at the position (u_1, u_2). The same procedure is repeated along the columns of the image to detect singularities.
Horizontal and vertical detected singularities are chained together to form edge curves. Figure 1 (b) shows a family of curves detected along each row and column of the noisy image in Figure 1 (a). This

(a) (b)

Fig. 1. (a) noisy image, (b) edge curves detected along each row and column

representation will guide the snake deformation toward the edges of the image.

3. ACTIVE CONTOUR METHODS: SNAKES

3.1. The Traditional Approach

An active contour is a deformable continuous curve

$$X(s) = [x_1(s), x_2(s)], s \in [0, 1] \tag{4}$$

that moves through the spatial domain of an image I to minimize an energy functional E. The energy E associated with the curve is a weighted sum of internal and external energies [3] [8]

$$E = \alpha E_{\text{int}} + \beta E_{ext} \tag{5}$$

The internal energy of a snake measures the desired properties of a contour's shape. In order to obtain smooth and physically feasible results, an elasticity and smoothness constraint are used in the energy functional. The smoothness constraint is, in general, based on the curvature of the active contour, which may be computed analytically from the properties of the contour. Then the internal energy is defined as follows:

$$E_{\text{int}} = \left(\oint_s \left(\left\|X(s)'\right\|^2 + \left\|X(s)''\right\|^2\right) ds\right) \left(\oint_s \left\|X(s)'\right\| ds\right) \tag{6}$$

Where $\|X(s)'\|^2$ and $\|X(s)''\|^2$ denote the first and second derivative of the curve with respect to s, and are measures for respectively the elasticity and smoothness. Measures independent of the spatial scale are obtained by multiplying the shape measure with the length of the contour.
The external energy is derived from the image in such a way that the snake is attracted to certain image features. Definitions of external energy are, amongst others, based on the image intensity, $I(x, y)$ or on the intensity of the Gaussian smoothed image. However, in most snake-type techniques the intensity gradient is considered as the primary image feature, leading to the following external term:

$$E_{ext} = \oint_s -\|\nabla I(x_1, x_2)\| ds \tag{7}$$

Where the gradient image $\|\nabla I(x, y)\|$ is usually derived from the intensity image through Gaussian smoothed derivatives.

3.2. Color Snake

A color image (R, G, B) can be considered as a function which maps a two dimensional spatial information to a three dimensional color space. The gradient of this field can be generalized to the derivatives of the vector field. The principled way to compute gradients in vector images as described by Silvano di Zenzo [9] and further used in [10] and [11] is summarized as follows.
Let $I(x_1, x_2)$:$\mathbb{R}^2 \to \mathbb{R}^m$ be an m-band image with components for $I_i(x_1, x_2) : \mathbb{R}^2 \to \mathbb{R}$ for $i = 1, 2, 3, ..., m$ ($m = 3$ for color images). Hence, at a given image location the image value is a vector in $\mathbb{R}^m$. The difference at two nearby points $A = (x^0_1, x^0_2)$ and $B = (x^1_1, x^1_2)$ is given by $\Delta I = I(A) - I(B)$. Considering an infinite small displacement, the difference becomes the differential $dI = \sum_{i=1}^{2} \frac{\partial I}{\partial x_i} dx_i$ and its squared norm is given by:

$$\begin{aligned} dI^2 &= \sum_{i=1}^{2}\sum_{j=1}^{2} \frac{\partial I}{\partial x_i}\frac{\partial I}{\partial x_j} dx_i dx_j = \sum_{i=1}^{2}\sum_{j=1}^{2} g_{ij} dx_i dx_j \\ &= \begin{bmatrix} dx_1 \\ dx_2 \end{bmatrix}^T \begin{bmatrix} g_{11} & g_{12} \\ g_{21} & g_{22} \end{bmatrix} \begin{bmatrix} dx_1 \\ dx_2 \end{bmatrix} \end{aligned} \tag{8}$$

Where $g_{ij} = \frac{\partial I}{\partial x_i}\frac{\partial I}{\partial x_j}$ and the extrema of the quadratic form are obtained in the direction of the eigenvectors of the matrix $[g_{ij}]$ and the values at these locations correspond with the eigenvalues λ_+ and λ_-. The eigenvectors provide the direction of maximal and minimal changes at a given point in the image, and the eigenvalues are the corresponding rates of change. Therefore, an approximation of edges for vector-valued images should be function $f = f(\lambda_+, \lambda_-)$. Since a function of the type $f = f(\lambda_+, \lambda_-)$ becomes the vector-image replacement of $\|\nabla I\|$ for singled-valued images ($m = 1$), traditional snake approach defined in (6) and (7) can be basically extended to vector-images by replacing the norm of the gradient with $f = f(\lambda_+, \lambda_-)$.

4. FOVEAL WAVELET-BASED COLOR SNAKE

We define a continuous foveal wavelet snake on a plane $S\vec{F}$ defined in turm of the foveal wavelet coefficients.

$$S\vec{F} \equiv \begin{pmatrix} SF^1\left(t, \vec{w}^1\right) \\ SF^2\left(t, \vec{w}^2\right) \end{pmatrix} \tag{9}$$

$$SF^i\left(t, \vec{w}^i\right) \equiv c^i + \sum_{j,k \in Z} \vec{w}^i_{j,k}\psi^i_{j,k}(t), i = 1, 2 \tag{10}$$

where $t \in [0, 1)$ is a contour parameter of the snake and $\vec{w}^i$ are the foveal wavelet coefficients ($\vec{w}^1$ for the vertical coefficients and $\vec{w}^2$ for the horizontal coefficients). c^i is the mean value of SF^i.
The deformation of the foveal wavelet snake is performed in a model-based manner. In this work, the foveal wavelet edge representation, described in the previous section, is used to guide the snake deformation.
Therefore, the image is considered as composed of background and one object of interest, each of which having unique properties represented by descriptors V_{out} and V_{in} respectively. For a given image domain Ω, let us define the following general criterion

$$J(\Omega) = \alpha \int_{\Omega_{in}} V_{in}(\Omega_{in}, \mathbf{x})\, d\mathbf{x} + \beta \int_{\Omega_{out}} V_{out}(\Omega_{out}, \mathbf{x})\, d\mathbf{x} \tag{11}$$

Where α and β are positive constants, Ω_{in} and Ω_{out} are the inside and outside domain of the object ($\Omega = \Omega_{in} \cup \Omega_{out}$). V_{in} and V_{out} are positive functions such that V_{in} is minimum in the object, i.e.

$$V_{in}(\Omega_{in}, \mathbf{x}) = (\mu(\Omega_{in}) - I(\mathbf{x}))^2 \tag{12}$$

where μ is the mean intensity

$$\mu(\Omega_{in}) = \frac{\int_{\Omega_{in}} I(\mathbf{x})\, d\mathbf{x}}{\int_{\Omega_{in}} d\mathbf{x}} \tag{13}$$

V_{out} is minimum in the background, meaning that no specific information is available for the background.

$$V_{out}(\Omega_{out}, \mathbf{x}) = (\mu(\Omega_{out}) - I(\mathbf{x}))^2 \tag{14}$$

If T represents the model image described above, and a foveal wavelet snake is placed on this image ($T = V_{in} \cup V_{out}$), there are three possibilities for the value of J:

- If the snake is completely confined inside Ω_{in}, the value of the cost function J is greater than zero because the value of the first integral is equal to zero whereas the second is greater than zero.
- If the snake is completely outside Ω_{in}, the value of t he cost function J is also greater than zero because the first integral is greater than zero and the second is equal to zero.
- If the snake fits the boundary of the two regions Ω_{in} and Ω_{out}, the cost function J becomes zero, because both integrals will be equal to zero.

Therefore, the minimum of criterion (11) is reached if Ωin segments the object of interest.
In this work, we used the foveal wavelet edge representation at a particular scale as a given image T. In other words, the foveal wavelet snake was used to fit the edges for estimating the boundary of the object of interest.
The minimization of the cost function J can be performed by updating the foveal wavelet coefficients $w^i_{j,k}$ in equation (10) by using the gradient descent algorithm as follows (it is to be noted that J is a function of Ω, which in turn is a function of $w_{j,k}$):

$$w^i_{j,k} \leftarrow w^i_{j,k} - \eta \frac{\partial J}{\partial w^i_{j,k}} \tag{15}$$

Where η is a small constant specifying the step size in the gradient descent algorithm. In a closed form, the partial derivative $\frac{\partial J}{\partial w^i_{j,k}}$ can be written as:

$$\frac{\partial J}{\partial w^i_{j,k}} = \left[W\left(j\frac{\partial SF^1}{\partial t}\right)\right]_{j,k} - \left[W\left(j\frac{\partial SF^2}{\partial t}\right)\right]_{j,k} \tag{16}$$

Where $[W(f)]_{j,k}$ indicates the foveal wavelet coefficient of f at a scale j and a position k.
It is to be noted that this derivative could be computed using the fast wavelet transform. In fact, by using (12) and (14) we can rewrite the cost function J as follows:

$$\begin{aligned} J &= \int_{\Omega_{in}} V_{in} d\mathbf{x} + \int_{\Omega_{out}} V_{out} d\mathbf{x} \\ &= \int_{\Omega_{in}} (V_{in} - V_{out})\, d\mathbf{x} + \left[\int_{\Omega_{in}} V_{out} d\mathbf{x} + \int_{\Omega_{out}} V_{out} d\mathbf{x}\right] \\ &= \int_{\Omega_{in}} (V_{in} - V_{out}) d\mathbf{x} + \int_{\Omega} V_{out} d\mathbf{x} \end{aligned} \tag{17}$$

Because the second term in (17) is a constant, we denote that turm by

$$C \equiv \int_{\Omega} V_{out} d\mathbf{x} \tag{18}$$

Because C is a constant, the partial derivative of J with respect to a foveal wavelet coefficient $w^i_{j,k}$ is equal to:

$$\frac{\partial J}{\partial w^i_{j,k}} = \int_0^1 (V_{in} - V_{out})\, |J|\, dt \tag{19}$$

Where $|J|$ is a Jacobian for the change of parameters, which is defined by

$$|J| = \begin{vmatrix} \frac{\partial SF^1}{\partial t} & \frac{\partial SF^2}{\partial t} \\ \frac{\partial SF^1}{\partial w^i_{j,k}} & \frac{\partial SF^2}{\partial w^i_{j,k}} \end{vmatrix} = \frac{\partial SF^1}{\partial t}\frac{\partial SF^2}{\partial w^i_{j,k}} - \frac{\partial SF^1}{\partial w^i_{j,k}}\frac{\partial SF^2}{\partial t} \tag{20}$$

We assume the mean values of the wavelet coefficients to be zero and that the foveal wavelet coefficients are orthogonal, we can obtain the following equation:

$$\frac{\partial SF^l}{\partial w^i_{j,k}} = \frac{\partial}{\partial w^i_{j,k}}\left\{\sum_{p,q} w^i_{p,q}\psi^l_{p,q}\right\} = \psi^l_{j,k} \tag{21}$$

Substituting (20) and (21) into (19), we obtain the closed form (16). Therefore, the computation of the snake deformation is made less expensive compared to the traditional snake approach which involves computationally expensive energy minimization process.
Another advantage is that the smoothness of the snake can be controlled by selecting appropriate wavelet scale.

5. EXPERIMENTAL RESULTS

This section is devoted for the evaluation of the foveal snake approach. To achieve this, we apply the traditional snake approach and the foveal wavelet snake approach to the noisy image in figure 2(b). The noisy image was obtained by adding a white gaussian noise with a variance of 0.2 to the image of figure 2(a). The corresponding edge representation of the noisy image obtained by the scheme described in section 2 is shown in figure 3.

(a) (b)

Fig. 2. (a) Original House image, (b) Noisy image

Fig. 3. (a) Edge representation obtained by using the foveal wavelet

The results of the active contour segmentation using the traditional snake approach (detailed in section 3) and the foveal wavelet based snake are shown in figures 4(a) and 4(b) respectively (the number of iterations is fixed to 500 for both experiences).
The initial snake in each case was a square at the edge of the image. A simple subjective examination clearly demonstrates that the foveal snake approach can identify objects boundaries in spite of the presence of noise.

6. CONCLUSION

A foveal wavelet based active contour was proposed. It integrates the foveal wavelet high accuracy edge representation with the traditional snake approach in order to achieve a noise invariant contour based segmentation.

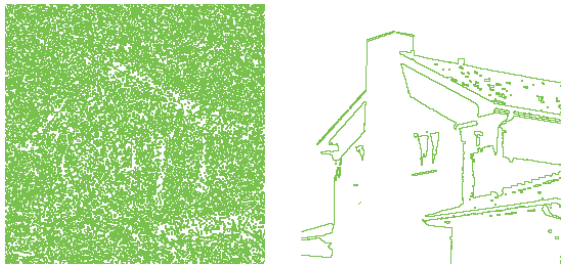

(a) (b)

Fig. 4. (a) Traditional Snake approach described in section 3 and extended to color image as explained in section 3.2, (b) Foveal wavelet snake approach

Further investigations for a complete characterization of the capture range of the foveal wavelet coefficients would help in snake initialization procedure. Perhaps, finding a way to automatically choose an optimal wavelet scale could help in these investigations.

7. REFERENCES

[1] S. Mallat, "Foveal orthonormal wavelets for singularities," Technical report, Ecole Polytechnique, 2000.

[2] S. W. Zucker, "Region growing: Childhood and adolescence (survey)," *Comp. Vision Graph. and Image Proc.*, vol. 5, pp. 382–399, 1976.

[3] A. Witkin M. Kass and D. Terzopoulos, "Snakes: Active contour models," *International Journal of Computer Vision*, vol. 1, no. 4, pp. 321–331, 1988.

[4] L. D. Cohen, "On active contour models and balloons," *CVGIP: Image Understanding*, vol. 53, no. 2, pp. 211–218, 1991.

[5] F. Leymarie and M. D. Levine, "Tracking deformable objects in the plane using an active contour model," *IEEE trans. on Pattern Anal. Machine Intell.*, vol. 15, no. 6, pp. 617–634, 1993.

[6] J. L. Prince and C. Xu, "A new external force model for snakes," *Image and multidimensional signal processing workshop*, pp. 30–31, 1996.

[7] C. Xu and J. L. Prince, "Snakes, shapes and gradient vector flow.," Technical report, The Johns Hopkins University, 1996.

[8] C. Xu and J.L. Prince, "Gradient vector flow: A new external force for snakes," *IEEE Proc. Conf. on Comp. Vis. Patt. Recog.*, pp. 66–71, 1997.

[9] S. di Zenzo, "A note on the gradient of multi-images," *Computer Vision Graphics and Image processing*, vol. 33, pp. 116–125, 1986.

[10] H. C. Lee and D. R. Cok, "Detecting boundaries in a vector field," *IEEE trans. on signal processing*, vol. 39, no. 5, pp. 1181–1194, 1991.

[11] G. Sapiro, "Color snakes," Technical report, Hewlett Packard Labs, 1995.